The Investigation on the Curing Process of Polysulfide Sealant by In Situ Dielectric Analysis

Baijie Zhou, Dan He, Yiwu Quan, Qingmin Chen

Polymer Science and Engineering Department, School of Chemistry and Chemical Engineering, State Key Laboratory of Coordination Chemistry, Nanjing University, Nanjing 210093, People's Republic of China

Received 17 March 2011; accepted 12 January 2012
DOI 10.1002/app.36813
Published online in Wiley Online Library (wileyonlinelibrary.com).

ABSTRACT: In this work, in situ dielectric analysis (DEA) was employed for the first time to the best of our knowledge, to monitor the curing process of polysulfide (PSF) sealant using manganese dioxide (MnO_2) as the curing agent, where the gel point and ending point were determined. The obtained results were verified by rheological tests of dynamic mechanical analysis and tensile strength tests. It showed a significant difference between this curing process and those of usual thermosetting materials. The influences of the pH value of the samples and curing temperature were investigated and discussed in detail. Also, activation energies of the curing reaction of the samples with different pH values were calculated. The results proved DEA as a reliable and useful method for in situ monitoring PSF–MnO_2 curing process. © 2012 Wiley Periodicals, Inc. J Appl Polym Sci 000: 000–000, 2012

Key words: polysulfides; curing of polymers; dielectric properties

INTRODUCTION

As the development of the low-molecular-weight polysulfide (PSF) resins bearing thiol end-groups in 1940, the crosslinked elastomers derived from PSF have found wide applications in industry, particularly those used as sealants. These materials are remarked by their excellent adhesion to glass, steel, wood, and concrete; their good low-temperature properties and low water-vapor permeability, and their high resistance to UV radiation and environment.[1,2] Most of the curing agents for PSF are metal peroxides, which oxidize the thiol group in PSF to cause crosslinking. A large quantity of relevant reactions for PFS crosslinking were reported.[3,4] Many publications can also be found on the characterization of PSF sealants, by the use of thermogravimetry analysis, dynamic mechanical analysis (DMA), tensile strength, and hardness testing.[5–9] In our previous study, chemical modification of PSF-based sealants has been studied to yield an improved mechanical property.[10–13]

In industrial applications, the curing process of PSF by metal peroxides is often influenced by many factors,[5,9,14] including the curing temperature, the quantity, and granularity of metal oxide, the type and amount of catalyst, and so on. It is difficult to monitor the curing process of PSF by infrared spectrum and differential scanning calorimeter, because of the weak infrared signal change before and after the reaction and low-reaction heat release. ERP and NMR spectroscopy were used by Coates et al.[4] to study the reaction mechanism of the PSF–MnO_2 curing process.[4] The gel point and hardness variation were investigated by Donaldson et al. to evaluate the curing rate.[9] Dielectric analysis (DEA) is based on the study of the dielectric response of a polymer. Its application to curing processes is sensitive to the mobility of ions and the rotation of dipoles in polymer structures. The important information obtained by DEA includes permittivity, dielectric loss, relative ion viscosity, curing rate, and the ending point of curing.[15] The dielectric behavior of thermosetting materials in curing process was reviewed by Senturia and Sheppard.[16] More attention, up to now, has paid to epoxy–amine system, but not to PSF–MnO_2 one.

In this article, DEA was used for the first time to investigate PSF–MnO_2 curing system. The gel point on DEA curve was determined and verified by DMA rheological method; the ending point occurred when $d\mathrm{Log}\varepsilon''/dt$ was close to 0, attaining 73.0 ± 1.5% tensile strength compared with the completely cured samples. The influences of the pH value and curing temperature on the curing process were also studied by in situ DEA. The activation energies (E_a) of the reaction for the samples with different pH values were calculated. The E_a of sample pH 3.4 is about 71.4 kJ/mol, whereas that of sample pH 7.9 is about 49.8 kJ/mol. The sample with a lower pH value has longer induction time and is more sensitive to the curing temperature.

Correspondence to: Q. Chen (chenqm@nju.edu.cn).

TABLE I
The Typical Compositions of Polysulfide Sealants

Materials	JLY121	JLY155	JLY124	Plasticizer	MnO_2	SFR black	SiO_2	DGEBA	KH560
Weight (g)	33	34	33	9	6	50	5	6	3

EXPERIMENTAL

Materials

Low-molecular-weight liquid PSF resins (JLY121: SH% = 6.2–7.5%, $M_n = 1000 \pm 200$, with 2% mol trithiol; JLY124: SH% = 1.6–2.0%, $M_n = 4000 \pm 200$, with 2% mol trithiol; JLY155: SH% = 1.0–1.4%, $M_n = 5000 \pm 400$, with 0.5% mol trithiol) were supplied by Jingxi Research Institute of Chemical Industry, China. MnO_2, carbon black (SFR, N774), silicon dioxide, dibutyl phthalate, sodium hydroxide (NaOH), an epoxy resin (DGEBA, a low-molecular-weight liquid diglycidyl ether of bisphenol A with epoxide value of 0.44) and a coupling agent (2,3-epoxypropoxy)propyltrimethoxysilicane, KH560, were all commercially available materials and used as received.

Preparation for MnO_2 with different pH values

MnO_2 with different pH values was prepared according to the literature.[9] At first, the powder of MnO_2 was mixed with deionized water to form a 5 wt % suspension, then NaOH solution of 1 mol/L was added into the suspension under magnetic stirring until the desired pH value was reached. During this procedure, oxygen was bubbled through the solution to prevent the reduction of the substance from air. The precipitate was separated from the solution, and then dried at 100°C and milled to uniform powder. The final pH values of obtained MnO_2 were 3.4, 4.6, 5.4, 6.5, and 7.9, respectively, and the corresponding sealant samples were marked as pH 3.4, 4.6, 5.4, 6.5, and 7.9.

Preparation of PSF sealant

The typical compositions of PSF sealants based on different fillers are listed in Table I. The liquid PSF resins, fillers, and curing agents were fully mixed by a mechanical stirrer and degassed by a Siemens DAC 150FV high-speed mixer at 3000 r/min (produced by Hauschild, Herrliberg, Germany).

Dielectric analysis

The curing process was monitored by a dielectric analyzer (NETZSCH DEA 230/1 Cure Monitor) controlled by a microcomputer with the planar wafer-thin sensor inserted into the reactor. The sensor was inert and has 2 cm × 1 cm in area and 0.5-mm thick. The electrode configuration was set in the reactor so as to be swept by the axial flow generated by the propeller.

Mechanical property

The mechanical properties of samples were measured on an Instron 4466 Universal Materials Testing Machine (Produced by Instron, Norwood, MA) with a speed of 50 mm/min at 23°C. The cured film in 2 mm thickness was cut into dumbbell-shaped specimens. Each result was obtained by a test repetition with three specimens.

DMA rheological test

The rheological measurements were carried out with a DMA + 450 (produced by 01 dB-Metravib, France), which employed a pasty liquid shear specimen-holder comprising a piston connected to a electrodynamic vibrator and a cup fixed at the bottom. After the mixed sample was introduced into the cup, the shear piston was inserted into the sample. The inside diameter of the cup was 10 mm, and the 15-mm immergence depth of the piston was kept. During the test, sinusoidal shear force was applied to the curing samples, and the response from the sample was monitored by detector.

RESULTS AND DISCUSSION

The DEA curves of the curing process of PSF–MnO_2

The DEA results response to various dielectric properties, such as permittivity, dielectric loss factor, and ion viscosity, where dielectric loss factor (ε'') is one of the most important parameters used to determine the curing degree.[17] This value was calculated from the monitored electric current and phase angle signals, comprising two components as expressed in eq. (1):

$$\varepsilon'' = \varepsilon''_{rd} + \frac{\sigma}{\omega\varepsilon_0} = \varepsilon''_{rd} + \frac{1}{\eta\omega\varepsilon_0} \quad (1)$$

where ε''_{rd} is the loss factor of the dipole orientation, σ is the ion conductivity, ω is the frequency of the electrical field, ε_0 is the vacuum dielectric constant, and η is the ion viscosity.

Figure 1(a) shows typical time variations of dielectric loss factor of the curing process of PSF–MnO_2 at 25°C. Usually, the value of ε'' decreases during the

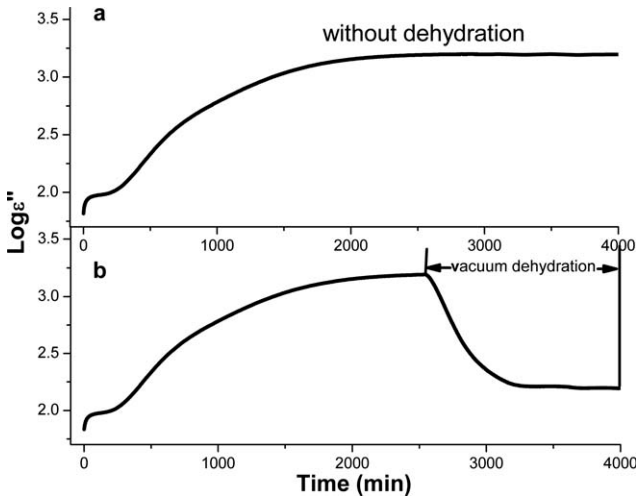

Figure 1 The Logε''–t curves of sample pH 3.4, (a) cured at 25°C for 4000 min; (b) cured at 25°C for 2500 min and then under vacuum dehydration at 25°C for another 1500 min.

curing process for common thermosetting plastics, as the two parts of ε'' are increasingly restricted as the crosslinking progress. However, Figure 1(a) shows that the ε'' increases all the time during the curing of liquid PSF, which was caused by the oxidation of thiol group. We believe that this phenomenon is related to the water release during the oxidation of liquid PSF as shown in Scheme 1. The released water increased the mobility of ions in the sample, leading to a rapid increase of the ε'' value in the initial 1500 min and reaches maximum at around 2500 min, corresponding to the formation of a solid state.

To prove the role of water, a dehydration experiment was carried out: first, sample pH 3.4 was cured at 25°C for 2500 min until the ε'' curve leveled off, and then the sample was dehydrated under vacuum at 25°C for another 1500 min [Fig. 1(b)]. The results revealed that there was a tremendous decrease in the ε'' after dehydration, because of the ion conductivity decreased during the dehydration owing to the loss of water. As controlled, Logε''–t curve of the sample without vacuum dehydration remained almost unchanged.

Commonly, the permittivity is also an important parameter for studying the curing process of a thermoset, such as epoxy–amine resin. Figure 2 shows the Logε'–t and Logε''–t curves of pH3 .4 and pH 7.9

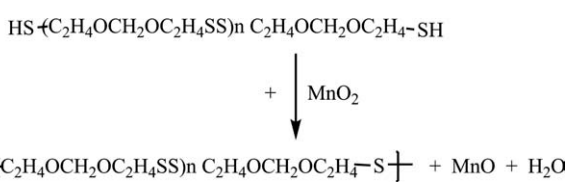

Scheme 1 Crosslinking by the oxidation of liquid PSF by manganese dioxide.

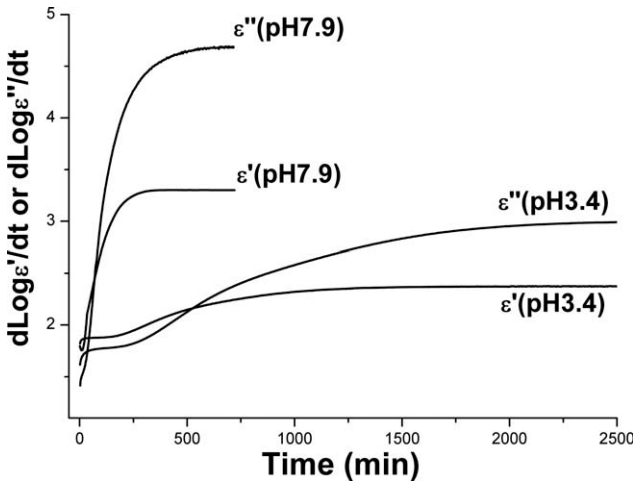

Figure 2 The variation of ε' and ε'' with curing time of samples pH 3.4 and pH 7.9 during curing at 25°C.

samples. It can be easily found that ε' curve leveled off much earlier than ε'', much earlier than the completion of the curing reaction. We believe this phenomenon is related to the fact that the value of ε' is more dependent on the mobility of the ions and small molecules in the PSF–MnO_2 curing system. With the raising of water quantity during the curing, the ion mobility could be promoted. Meanwhile, the increased molecular weight and crosslinking density of the polymer, which became more pronounced at the later period of the curing process, will reduce the ion mobility. The competition of these two effects resulted in the ε' value increasing in early stage and leveled off later. However, the value of ε'' is related to the energy loss caused by the movement of dipole and ion, it will keep increasing until glass transition point is researched. As the glass transition temperature of the PSF rubber is lower than room temperature, the Logε''–t curve will keep increasing during the curing process at a temperature higher than the glass transition temperature.

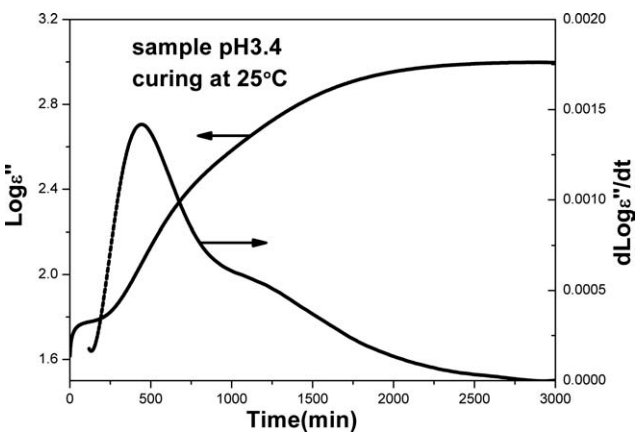

Figure 3 Logε''–t and dLogε''/dt–t curves of sample pH 3.4 cured at 25°C, 1 KHz.

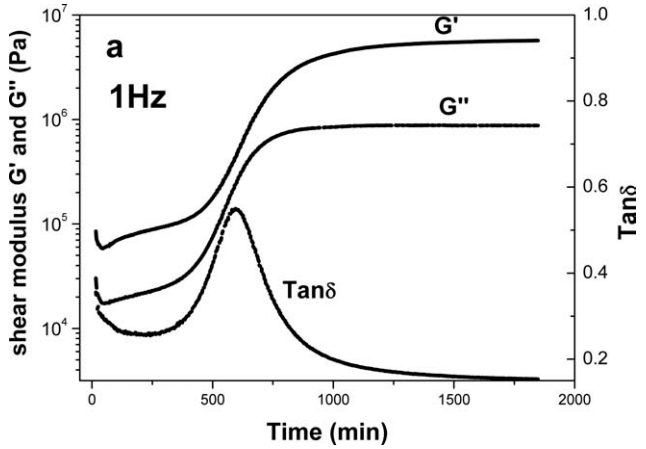

Figure 4 DMA rheological curves of sample pH 3.4 cured at 25°C.

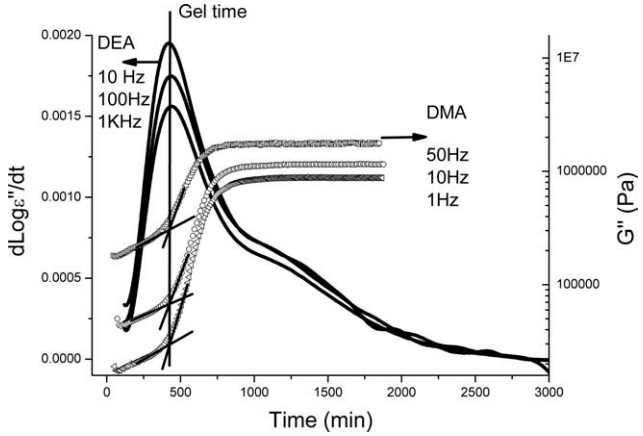

Figure 5 $d\text{Log}\varepsilon''/dt$–$t$ curves and LogG''–t curves of sample pH 3.4 at different testing frequencies.

The determination of gel point

It was suggested to take the peak position of Logε''–t curve as the gel time for epoxy–amine curing system, and the results showed that the value did not depend on the test frequencies.[17,18] However, as mentioned above, for PSF–MnO_2 system, the peak on Logε''–t curve will not appear owing to the glass transition temperature of the cured PSF rubber lower than room temperature. Therefore, the first-order derivation curve of Logε'' of sample pH 3.4 ($d\text{Log}\varepsilon''/dt$–$t$) is plotted in Figure 3. This curve showed a peak at $\sim$ 450 min corresponding to the maximum increasing rate in the Logε''–t curve, denoting the maximum increasing of energy loss owing to the chain movement. After then, there is a quick decrease of the $d\text{Log}\varepsilon''/dt$ value from 450 to 850 min, and thereafter this value reduces to 0 gently as the consequence of the completion of the curing process.

As the curing process progressed, the polymer chain reduced its moving capability. The reduction of the chain mobility would reach the highest speed around the gel point. This characteristic is exactly correlated with the appearance of peak in $d\text{Log}\varepsilon''/dt$–$t$ curve. Therefore, we believe that the peak position of the $d\text{Log}\varepsilon''/dt$–$t$ curve should correspond to the gel point. To verify this hypothesis, DMA rheological experiments were carried out to monitor the shear modulus with curing time. Figure 4 shows the DMA results of sample pH 3.4 cured at 25°C, including shear storage modulus (G'), loss modulus (G''), and Tan loss angle (Tanδ). With the progress of the curing reaction, G' and G'' kept increasing, indicating that the molecular weight and crosslinking degree were increased. The $d\text{Log}\varepsilon''/dt$–$t$ curves from DEA tests and the LogG''–t curves from DMA test at the frequencies of 1, 10, and 50 Hz were replotted in Figure 5 for comparison. The Logε''–t curves portray a frequency-independent inflection point, at which a distinct slope change between the two linear parts was positioned. This point was considered as the gel point in the previous publications.[17,18] As shown in Figure 5, this inflection point of LogG''–t curve appears at the same position as the peak of the DEA derivation curves, which is also independent of the frequencies. Based on this observation, we can conclude that the peak position of the $d\text{Log}\varepsilon''/dt$–$t$ curve could be a good estimate of the gel point for the PSF–MnO_2 curing system.

The determination of curing degree

According to the literature,[19] the curing degree at a curing time t (CD(t)) can be estimated from dielectric loss factors (ε'') using eq. (2):

$$\text{CD}(t) = \frac{\log\varepsilon''(\text{initial}) - \log\varepsilon''(t)}{\log\varepsilon''(\text{initial}) - \log\varepsilon''(\text{end})} \times 100\% \quad (2)$$

where initial, t and end represent the curing time $t_{\text{cure}} = 0$, t and ∞. Logε''(end) was measured from

TABLE II
Curing Degree Calculated by Tensile Strength When $d\text{Log}\varepsilon''/dt \approx 0$

Sample pH 7.9 (°C)	The time when $d\text{Log}\varepsilon''/dt \approx 0$ (h)	Tensile strength when $d\text{Log}\varepsilon''/dt \approx 0$ (MPa)	Tensile strength after sufficient curing (MPa)	CD (%) from tensile strength when $d\text{Log}\varepsilon''/dt \approx 0$
15	26.0	2.6	3.50 (More than 20 days)	74.3
25	11.0	2.6		74.3
35	6.0	2.5		71.5
50	1.5	2.5		71.5

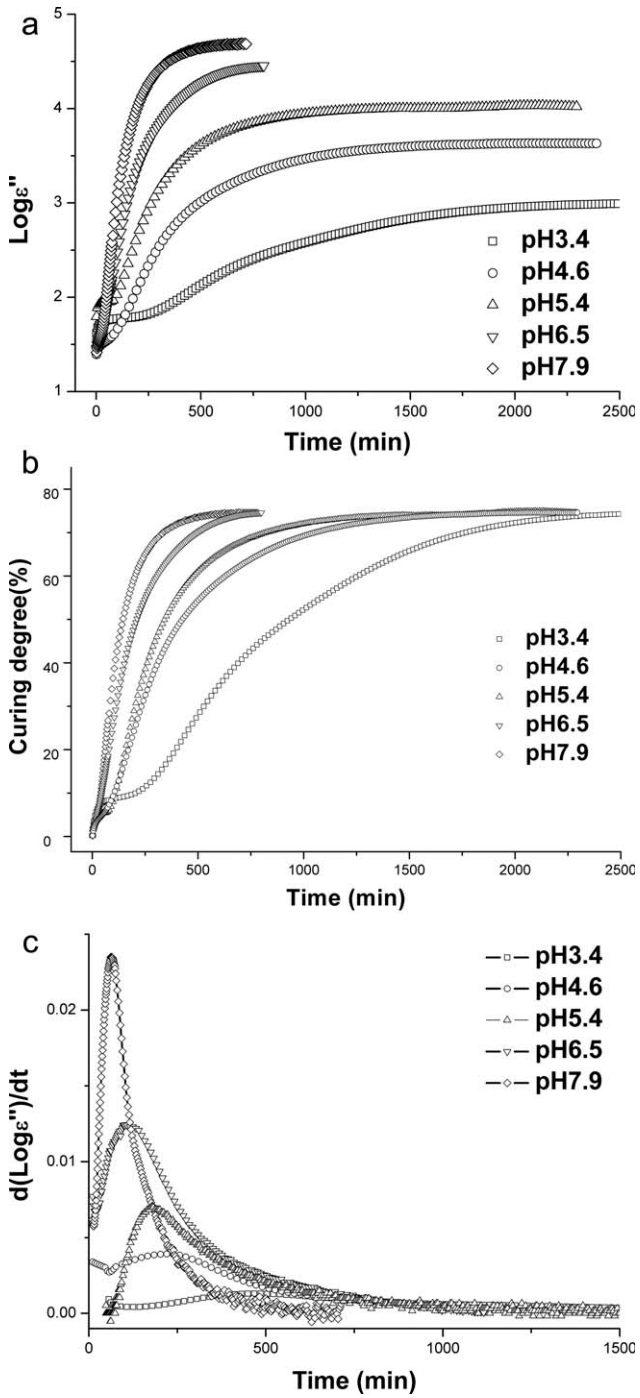

Figure 6 (a) Logε''–t, (b) curing degree, and (c) $d\text{Log}\varepsilon''/dt$ curves from the DEA test of the samples with different pH values cured at 25°C.

the curve when $d\text{Log}\varepsilon''/dt \approx 0$, which is assumed as the completion of the curing.

Actually, the curing degree had not reached 100% yet when the value of $d\text{Log}\varepsilon''/dt$ is close to 0, but the reaction after this point was very slow so that DEA method became insensitive. The actual curing degree at this point was investigated by a tensile strength test using sample pH 7.9 as an example. This sample showed the highest curing speed among all of the tested samples. The result is summarized in Table II. The result shows the actual curing degrees at the end of DEA tests when $d\text{Log}\varepsilon''/dt \approx 0$ was reached were about 73.0 ± 1.5%. Consequently, the final curing degree of DEA curves in the following discussion will be adjusted accordingly.

The influence of the pH on the curing process of PSF sealant

In an environment with a high pH value, the PSF thiol group is easy to lose the proton and turned to a thiolate. This anionic form has an increased electronegativity than the original neutral form and thus is prone to be oxidized by MnO_2. Therefore, the PSF sample with a higher pH value should have a higher curing speed than the one with a lower pH value. Figure 6 shows the pH dependence of the Logε''–t curves for the sample cured at 25°C, and the derived curing degree curves by eq. (2) and the $d\text{Log}\varepsilon''/dt$–$t$ curves. It can be seen that inflection stages (the period before the onset of Logε''–t curve) turned narrow and even disappeared as the pH value increased. The peak intensity of the $d\text{Log}\varepsilon''/dt$–$t$ curves also increased significantly with the increase of the pH value.

Figure 6 also indeed shows that the curing rate at 25°C is greatly depended on the pH value of the samples. Those with higher pH values displayed higher reaction rates. To compare the results of all the samples with different pH values and curing temperatures, the gel time and the ending time (the time when $d\text{Log}\varepsilon''/dt \approx 0$ reached) were extracted from the Logε''–t measurement using the method described above, and the result is summarized in Table III. It shows that the curing rate at a low temperature has higher pH dependence than the reaction at a high temperature. For example, the discrepancy of the gel time at 15°C between samples pH 7.9 and pH 3.4 was 9.0 times; however, it decreased to 3.1 times when the temperature increased to 50°C. As will be discussed in the following part, this phenomenon is attributed to the difference in the activation energy of the curing reaction of the samples with different pH values.

TABLE III
Gel Time and Ending Time of Samples At Different Curing Temperatures

Temp (°C)	Samples	pH 3.4	pH 4.6	pH 5.4	pH 6.5	pH 7.9
15	Gel time	1350	860	640	420	150
	Ending time	9000	5000	4000	3100	1600
25	Gel time	470	270	200	115	65
	Ending time	2300	1900	1700	800	650
35	Gel time	160	135	120	65	35
	Ending time	950	820	730	470	350
50	Gel time	50	36	27	20	16
	Ending time	230	160	140	110	100

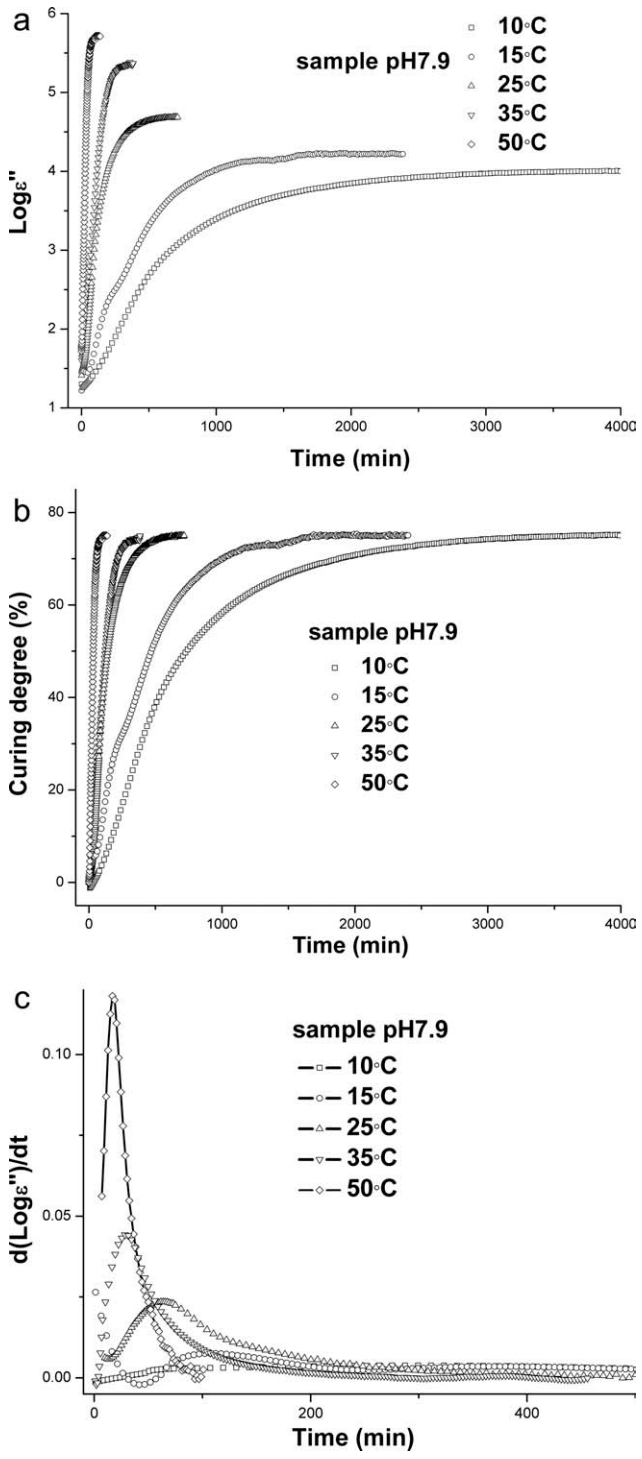

Figure 7 (a) Logε''–t, (b) curing degrees, and (c) $d\text{Log}\varepsilon''/dt$ curves from DEA of sample pH 7.9 cured at different temperatures.

The influence of the temperature on the curing process of PSF sealant

On the other hand, Table III also summarizes that the temperature dependence was weak for the sample with a high pH value, whereas strong for that with a low pH value. As an example, the gel time of sample pH 3.4 at 15°C is about 27 times longer than 50°C. However, the gel time of sample pH 7.9 at 15°C is only about nine times longer than 50°C. This phenomenon must indicate that the curing process of the samples with different pH values has different activation energies, which will be discussed later.

To discuss the temperature effect in detail, we plotted the experimental results of sample pH 7.9 cured at different temperatures in Figure 7 in which the curves of Logε'', curing degrees, and $d\text{Log}\varepsilon''/dt$ versus curing time are shown. In general, Figure 7 shows an increased curing rate, a significantly reduced induction time, and promoted peak intensity in $d\text{Log}\varepsilon''/dt$–$t$ curves with the increase of the curing temperature.

As mentioned above, two characteristic points can be derived from the Logε''–t curves. They are gel points corresponding to the peak position of the $d\text{Log}\varepsilon''/dt$–$t$ curve and the ending point appeared when $d\text{Log}\varepsilon''/dt$–$t$ was close to 0. The curing degree at the ending point was about 73.0% derived from the results of the tensile strength test (Table II). On the other hand, the data of Figure 7(b) are replotted in Figure 8 in which the curing degrees at the gel points were picked based on the obtained gel time of each sample, and marked with an open circle in the figure. It indicates that the curing degrees of sample pH 7.9 at different temperatures are all in scale of 23.5 ± 3%.

The activation energy of the curing process of PSF sealant with different pH values

To calculate the activation energy of the curing reaction of the PSF system, the differential expression of the activation energy in eq. (3) is adopted:

$$dx/dt = A\exp(-E_a/RT)f(x) \tag{3}$$

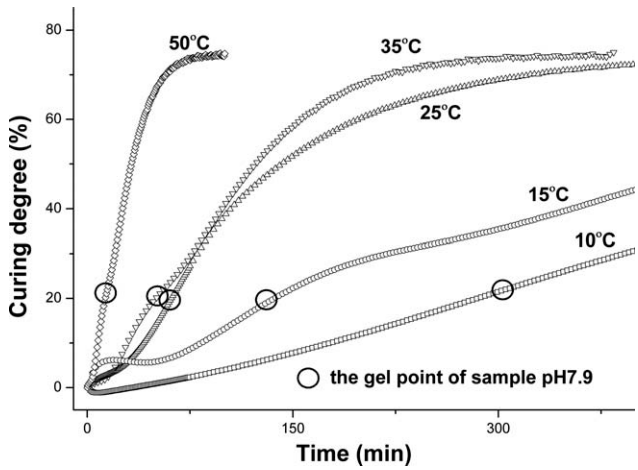

Figure 8 Curing degrees of sample pH 7.9 at different curing temperatures, with open circles indicating the gel points.

where R is the gas constant, T is the curing temperature, and $f(x)$ is the equation defined by the reaction mechanism, which is independent of the temperature.

For a certain reaction, activation energy E_a and the pre-exponential factor A should be constants. The integration of eq. (3) from the beginning at $t = 0$ to the time of a characteristic point $[t(P_C)]$ is expressed by eq. (4).

$$\ln \int_0^{t(m)} \frac{dx}{f(x)} = \ln A + \ln[t(P_C)] - \frac{E_a}{RT} \Rightarrow \ln(t(P_C)) = \text{constant} + E_a/RT \quad (4)$$

According to eq. (4), the curves of $\ln[t(P_C)]$ versus $1000/T$ can be depicted as shown in Figure 9. Figure 9(a,b) is based on the $t(P_C)$ of gel time and ending time, respectively. The slope of the fitting line is $E_a/1000R$ as given in eq. (4). The computed activation energies are listed in Table IV.

This result indeed indicates that a greater E_a of the sample with a lower pH value, meaning a higher sensitivity of the curing reaction to the temperature.

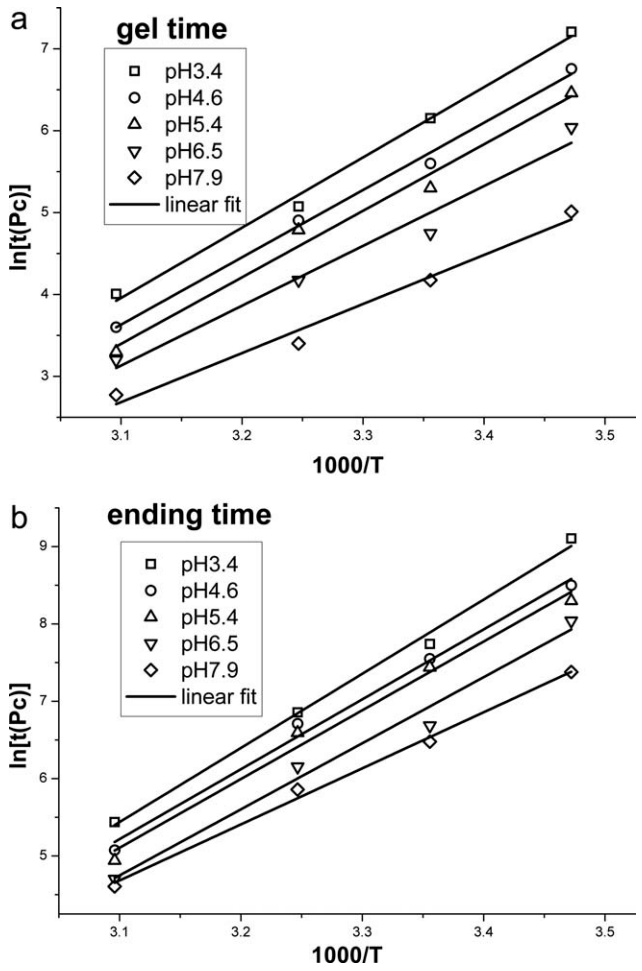

Figure 9 $\ln[t(P_C)]$ versus $1000/T$ curves of samples, the data points were derived from the experimental results as listed in Table III, and were fitted by eq. (4) (solid line).

TABLE IV
The Slope of Fitting Lines and the Activation Energies (kJ)

Sample	pH 3.4	pH 4.6	pH 5.4	pH 6.5	pH 7.9
Activation energy[a] (kJ/mol)	71.4	68.3	67.5	60.8	49.8
Activation energy[b] (kJ/mol)	79.7	75.1	73.9	71.0	60.3

[a] From gel time.
[b] From ending time.

The E_a of the samples with different pH values were in the range of 49.8–60.9 kJ/mol (sample pH 7.9) and 71.4–79.7 kJ/mol (sample pH 3.4). The phenomenon that E_a derived from gel time is smaller than that from ending time can be easy to understand. In the later period of the curing process, the formation of the crosslinked network will create resistance to the curing reaction, leading to a higher apparent activation energy. Therefore, we believe the E_a data from the gel point reflect more realistically the characteristics of the curing reaction.

CONCLUSIONS

1. DEA was successfully used to monitor the curing process of PSF–MnO_2. The gel point was derived from the peak position of $d\text{Log}\varepsilon''/dt$–$t$ curve, and the result was verified by DMA rheological tests. The ending point occurred when $d\text{Log}\varepsilon''/dt$ was close to 0, attaining 73.0 $\pm$ 1.5% curing degree derived from the tensile strength test.
2. The influences of pH and curing temperature on the PSF–MnO_2 curing process were prominent. At a higher temperature, the curing rate had a relatively weaker pH dependence. On the other hand, the sample with a higher pH value had a lower temperature dependence, indicating a smaller activation energy.
3. Based on the gel point and ending point derived from the DEA curves, activation energies were calculated. The E_a of the samples with different pH values were in the range of 49.8–60.9 kJ/mol (sample pH 3.4) and 71.4–79.7 kJ/mol (sample pH 7.9). The results had a good correspondence with the experimental phenomena.

The authors thank Prof. Jianfu Ding from Institute for Chemical Process and Environmental Technology, National Research Council Canada, and Prof. Xuehai Yu from School of Chemistry and Chemical Engineering, Nanjing University, for their helpful comments and modifications on this paper.

References

1. Ellerstein, S. In Encyclopedia of Polymer Science and Engineering, 2nd ed.; Mark, H. F., Bikales, N. W., Overberger, C. G., Menges, G., Eds.; Wiley: New York, 1988; Vol.1.
2. Ghatege, N. D.; Vernekar, S. P.; Lonikar, S. V. Rubber Chem Technol 1980, 54, 197.
3. Capozzi, G.; Modena, G. In Chemistry of the Thiol Group, Part 2, Patai, S., Ed.; Wiley: New York, 1974.
4. Coates, R. J.; Gilbert, B. C.; Lee, T. J Chem Soc Perkin Trans II 1992, 2, 1387.
5. Usmani, A. E. Polym Plast Technol 1982, 19, 165.
6. Krishnan, K.; Ninan, K. N. J Therm Anal 1986, 35, 1223.
7. Radhakrishnan, T. S.; Rama, R. M. J Appl Polym Sci 1987, 34, 1985.
8. Matsui, T.; Miwa, Y. J Appl Polym Sci 1999, 71, 59.
9. Donaldson, I. D.; Grimes, S. M.; Houlson, A. D.; Behn, S. J Appl Polym Sci 2000, 77, 1177.
10. Quan, Y. W.; Dong, W. Z.; Fang, J. L.; Chen, Q. M. J Appl Polym Sci 2004, 91, 2358.
11. Quan, Y. W.; He, P.; Zhou B. J.; Chen, Q. M. J Appl Polym Sci 2007, 106, 2599.
12. Lu, Y.; Shen, M. X.; Ding, X. D.; Quan, Y. W.; Chen, Q. M. J Appl Polym Sci 2010, 115, 1718.
13. Lu, Y.; Zhang, J. S.; Chang, P. S.; Quan, Y.W.; Chen Q. M. J Appl Polym Sci 2011, 120, 2001.
14. Honda, K.; Yonetani, H. The Durability of Sealing Compound for Rolling Stock; Kinki Sharyo: Japan. Nippon Setchaku Gakkai Nenji Taikai Koen Yoshishu, 37th, 1999.
15. Shepared, D. D.; Twombly, B. Thermochim Acta 1996, 272, 125.
16. Senturia, S. D.; Sheppard, N. F. Adv Polm Sci 1986, 80, 1.
17. Harper, D. P.; Wolcott, M. P.; Rials, T. G. Int J Adhes Adhes 2001, 21, 137.
18. Edith T. A. Thermal Characterization of Polymeric Materials, 2nd ed., Amazon, Academic Press: San Diego, London, 1997; Vol.2, Chapter 6.
19. Nunez-Regueira, L.; Gracia-Fernandez, C.A.; Gomez-Barreiro, S. Polymer 2005, 46, 5979.